3
Blood Flow in Arteries

3.1 Introduction

The larger systemic arteries, shown in Figure 3.1:1, conduct blood from the heart to the peripheral organs. Their dimensions are given in Table 3.1:1. In humans, the aorta originates in the left ventricle at the aortic valve, and almost immediately curves about 180°, branching off to the head and upper limbs. It then pursues a fairly straight course downward through the diaphragm to the abdomen and legs. The aortic arch is tapered, curved, and twisted (i.e., its centerline does not lie in a plane). Other arteries have constant diameter between branches, but every time a daughter branch forks off the main trunk the diameter of the trunk is reduced. Overall, the aorta may be described as tapered. In the dog, the change of area fits the exponential equation,

$$A = A_0 e^{(-Bx/R_0)},$$

where A is the area of the aorta, A_0 and R_0 are, respectively, the area and radius at the upstream site, x is the distance from that upstream site, and B is a "taper factor," which has been found to lie between 0.02 and 0.05. Figure 3.1:2 shows a sketch of the dog aorta.

If there is a fluid of sufficiently large quantity in static condition outside a blood vessel so that the blood vessel may be considered as an isolated tube bathed in a large reservoir, then at a given blood pressure the stress in the blood vessel wall depends on the radius and wall thickness of the vessel. These quantities change considerably with age (see, e.g., Fig. 3.1:3). Associated with these geometric changes are changes in elastic properties. In the thoracic aorta, at a physiological pressure of $1.33 \times 10^4\,\mathrm{Nm}^{-2}$ (100 mm Hg), the incremental Young's modulus E increases steadily with age; but in more peripheral vessels there is either no change or a fall [Fig. 3.1:4(a) and (b)]. The explanation for this appears to be that the diameter of the thoracic aorta increases with age, whereas that of the iliac and femoral arteries either decreases or changes little with age (see Fig. 3.1:3);

TABLE 3.1:1. Normal Values for Canine Cardiovascular Parameters

Site	Units	Ascending aorta		Descending aorta	Abdominal aorta	Femoral artery	Carotid artery	Arteriole	Capillary	Venule	Inferior vena cava	Main pulmonary artery
Internal diameter d_i	cm	1.5		1.3	0.9	0.4	0.5	0.005	0.0006	0.004	1.0	1.7
		1.0–2.4		0.8–1.8	0.5–1.2	0.2–0.8	0.2–0.8	0.001–0.008	0.0004–0.0008	0.001–0.0075	0.6–1.5	1.0–2.0
Wall thickness h	cm		0.065		0.05	0.04	0.03	0.002	0.0001	0.0002	0.015	0.02
			0.05–0.08		0.04–0.06	0.02–0.06	0.02–0.04				0.01–0.02	0.01–0.03
h/d_i			0.07		0.06	0.07	0.08	0.4	0.17	0.05	0.015	0.01
			0.055–0.084		0.04–0.09	0.055–0.11	0.053–0.095					
Length	cm	5		20	15	10	15	0.15	0.06	0.15	30	3.5
							10–20	0.1–0.2	0.02–0.1	0.1–0.2	20–40	3–4
Approximate cross-sectional area	cm^2	2		1.3	0.6	0.2	0.2	2×10^{-5}	3×10^{-7}	2×10^{-5}	0.8	2.3
Total vascular cross-sectional area at each level	cm^2	2		2	2	3	3	125	600	570	3.0	2.3
Peak blood velocity	$cm\ s^{-1}$	120		105	55	100		0.75	0.07	0.35	25	70
		40–290		25–250	50–60	100–120		0.5–1.0	0.02–0.17	0.2–0.5	15–40	
Mean blood velocity	$cm\ s^{-1}$	20		20	15	10						15
		10–40		10–40	8–20	10–15						6–28
Reynolds number (peak)		4500		3400	1250	1000		0.09	0.001	0.035	700	3000
α (heart rate 2 Hz)		13.2		11.5	8	3.5	4.4	0.04	0.005	0.035	8.8	15
Calculated wave speed c_o	$cm\ s^{-1}$		580		770	840	830				100	350
Measured wave speed c	$cm\ s^{-1}$		500		700	900	800				400	250
			400–600		600–750	800–1030	600–1100				100–700	200–330
Young's modulus E	$Nm^{-2} \times 10^5$		4.8		10	10	9				0.7	6
			3–6		9–11	9–12	7–11				0.4–1.0	2–10

An approximate average value, and then the range, is given where possible.
From Caro, Pedley, and Seed (1974). Reproduced by permission.

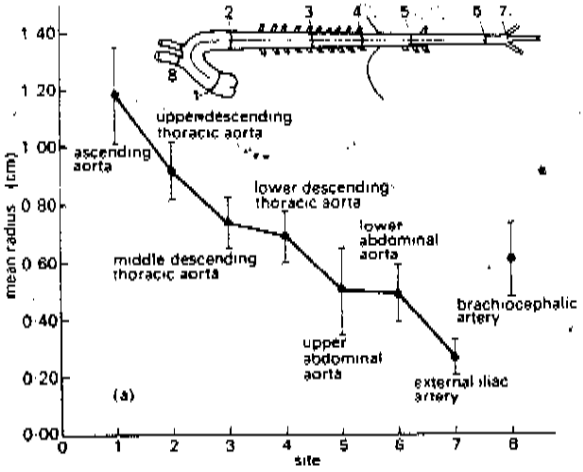

FIGURE 3.1:2. A sketch of the dog's aorta from data measured at physiological pressure in 10 large dogs. From Fry, Griggs, Jr., and Greenfield, Jr. (1964) In vivo studies of pulsatile blood flow. In *Pulsatile Blood Flow*, Attinger, (ed.). McGraw-Hill, New York, p. 110, by permission.

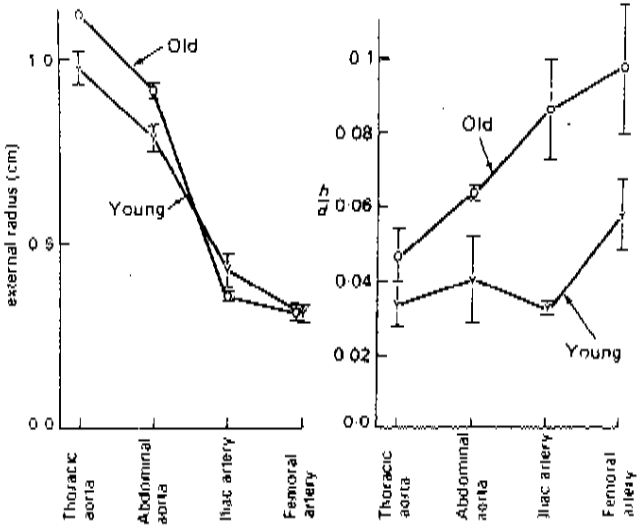

FIGURE 3.1:3. The radius and wall thickness of human arteries for young (Y) and old (O) persons. From Learoyd and Taylor, (1966) Alterations with age in the viscoelastic properties of human arterial walls. *Circ. Res.* **18**: 278–292, by permission of the American Heart Association.

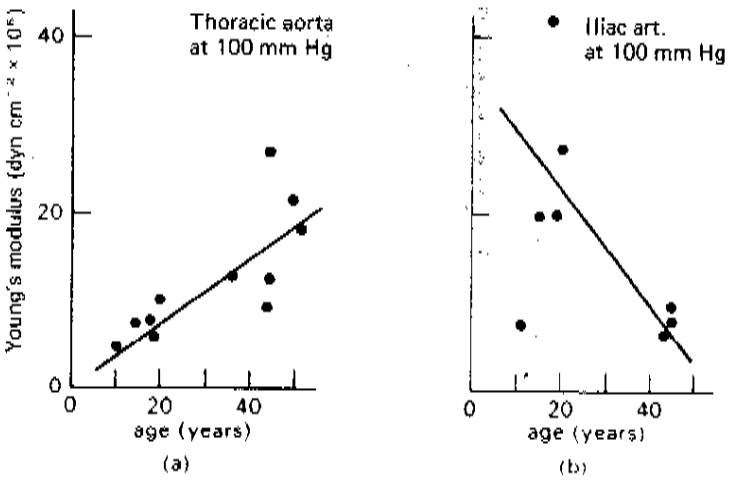

FIGURE 3.1:4. Incremental modulus of elasticity of arteries of normal young and old persons at a pressure of 100 mm Hg. (a) Thoracia aorta. (b) Iliac artery. From Learoyd and Taylor, (1966) *Circ. Res.* **18**: 278–292, by permission of the American Heart Association.

Tissues (Fung, 1993b, p. 270), or Figure 3.1:5 of this book, tells us that at higher stress the incremental Young's modulus is larger.

A detailed discussion of the mechanical properties of arteries is given in Chapter 8 of *Biomechanics: Mechanical Properties of Living Tissues* (Fung, 1993b). In the present chapter we consider the flow of blood in these elastic vessels. The basic equations of hemodynamics are presented in Section 2.6. In most organs, the tissue outside the blood vessel cannot be considered to be a static fluid reservoir. In the skeletal muscle and myocardium, the blood vessels are closely integrated with muscle cells. In the lung, the pulmonary arteries and veins are tethered by interalveolar septa. The interaction between a blood vessel and its surrounding tissues then becomes a major feature of the blood flow in organs. This will be illustrated in Chapters 6 to 8.

We proceed from the simple to the complex. First, we give a solution to the problem of steady flow in a uniform rigid pipe. It is interesting to see that this simple solution has important applications. We also see that even this simple case has some very difficult aspects, for example, the questions of stability and turbulence. We then proceed to study aspects of flow in elastic tubes, first steady flow and then wave propagation. Reflection and transmission of waves in branching vessels is a subject of major interest. This brings us to pulsatile flow in the arteries, nonlinear effects, flow separation, entrance flow, messages carried in the pulse waves, and finally, mechanics of atherogenesis.

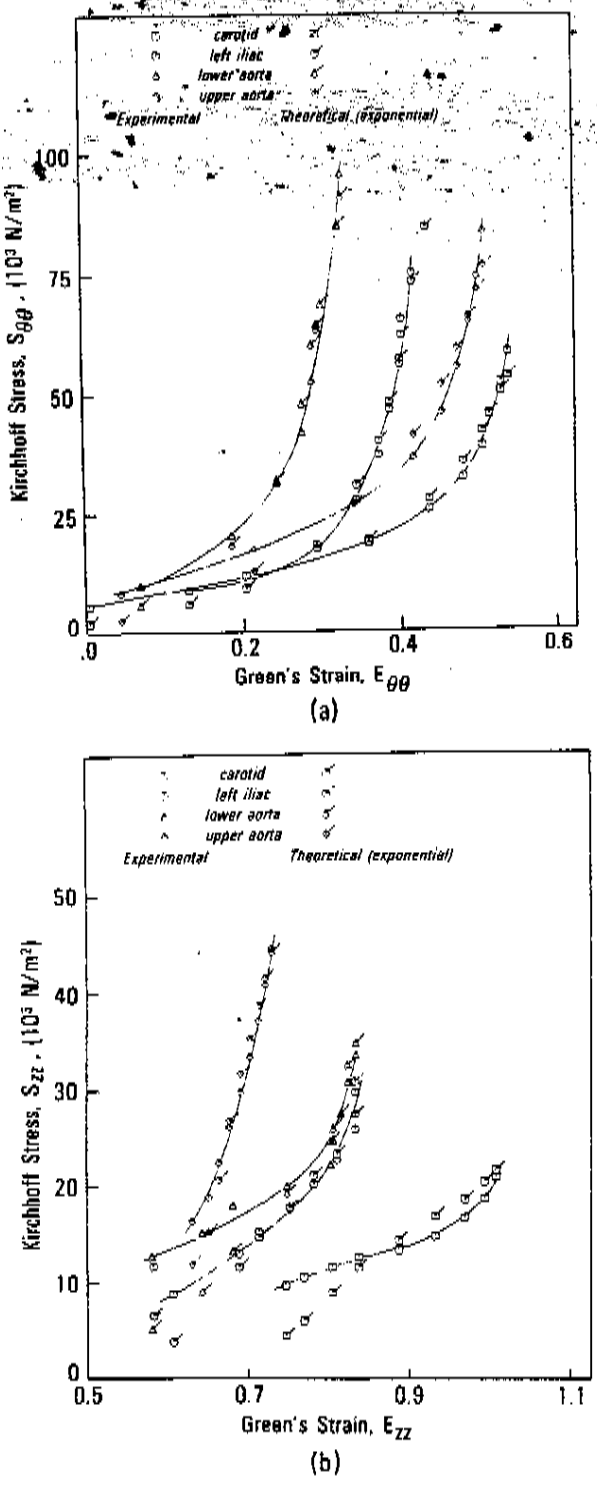

FIGURE 3.1:5. The stress–strain relationship of the thoracic aorta of the rabbit. From Fung, Fronek, and Patitucci (1979), by permission.

3.2 Laminar Flow in a Channel or Tube

Consider first a steady flow of an incompressible Newtonian fluid in a rigid, horizontal channel of width $2h$ between two parallel planes, as shown in Figure 3.2:1. The channel is assumed horizontal so that the gravitational effect (a body force) may be ignored. The walls are assumed to be so rigid that their geometry is uninfluenced by the flow. The coordinate system is shown in the figure, with x parallel to the wall.

With (u, v, w) denoting velocity, μ denoting the coefficient of viscosity, p the pressure, τ the shear stress, γ the shear strain rate, we search for a uniaxial flow with u the only nonvanishing velocity which is a function of y:

$$u = u(y), \quad v = 0, \quad w = 0, \tag{1}$$

The equation of continuity [Eq. (8) of Section 2.6],

$$\frac{\partial u}{\partial x} + \frac{\partial v}{\partial y} + \frac{\partial w}{\partial z} = 0$$

is satisfied by Eq. (1). The equations of motion [Eq. (13) of Sec. 2.6] which have been reduced to the Navier-Stokes equations [Eq. (18) of Sec. 2.6], now become

$$0 = -\frac{\partial p}{\partial x} + \mu \frac{d^2 u}{dy^2}, \tag{2}$$

$$0 = \frac{\partial p}{\partial y}, \tag{3}$$

$$0 = \frac{\partial p}{\partial z}. \tag{4}$$

The no-slip conditions on the boundaries $y = \pm h$ are

$$u(h) = 0, \quad u(-h) = 0. \tag{5}$$

Equations (3) and (4) show that p is a function of x only. If we differentiate Eq. (2) with respect to x and use Eq. (1), we obtain $\partial^2 p/\partial x^2 = 0$. *Hence $\partial p/\partial x$ must be a constant.* Equation (2) then becomes

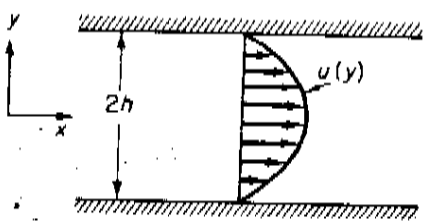

FIGURE 3.2:1. Laminar flow in a channel.

$$\frac{d^2u}{dy^2} = \frac{1}{\mu}\frac{dp}{dx}, \tag{6}$$

which has the solution

$$u = A + By + \frac{1}{\mu}\frac{y^2}{2}\frac{dp}{dx}. \tag{7}$$

The two constants A and B can be determined by the boundary conditions (2) to yield the final solution

$$u = -\frac{1}{2\mu}\left(h^2 - y^2\right)\frac{dp}{dx}. \tag{8}$$

Thus, the velocity profile is a parabola.

A corresponding problem is the flow through a horizontal circular cylindrical tube of radius a (Fig. 3.2:2). We search for a solution, as follows:

$$u = u\left(y, z\right), \quad v = 0, \quad w = 0.$$

In analogy with Eq. (6), the Navier–Stokes equation becomes

$$\frac{\partial^2 u}{\partial y^2} + \frac{\partial^2 u}{\partial z^2} = \frac{1}{\mu}\frac{dp}{dx}, \tag{9}$$

where dp/dx is a constant. For convenience we will use cylindrical polar coordinates x, r, θ, with $r^2 = y^2 + z^2$, instead of the cartesian coordinates x, y, z. Then Eq. (9) becomes

$$\frac{\partial^2 u}{\partial y^2} + \frac{\partial^2 u}{\partial z^2} = \frac{1}{r}\frac{\partial}{\partial r}\left(r\frac{\partial u}{\partial r}\right) + \frac{1}{r^2}\frac{\partial^2 u}{\partial \theta^2} = \frac{1}{\mu}\frac{dp}{dx}. \tag{10}$$

Let us assume that the flow is symmetric so that u is a function of r only; then $\partial^2 u/\partial\theta^2 = 0$, and the equation

$$\frac{1}{r}\frac{d}{dr}\left(r\frac{du}{dr}\right) = \frac{1}{\mu}\frac{dp}{dx} \tag{11}$$

can be integrated immediately to yield

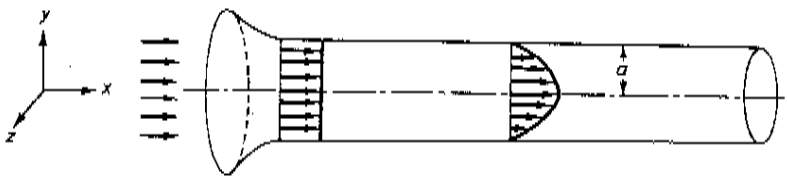

FIGURE 3.2:2. Laminar flow in a circular cylindrical tube.

$$u = \frac{1}{\mu}\frac{r^2}{4}\frac{dp}{dx} + A\log r + B. \tag{12}$$

The constants A and B are determined by the conditions of no-slip at $r = a$ and symmetry on the center line, $r = 0$:

$$u = 0 \quad \text{at} \quad r = a, \tag{13}$$

$$\frac{du}{dr} = 0 \quad \text{at} \quad r = 0. \tag{14}$$

The final solution is

$$u = -\frac{1}{4\mu}\left(a^2 - r^2\right)\frac{dp}{dx}. \tag{15}$$

This is the famous parabolic velocity profile of the *Hagen–Poiseuille flow*; the theoretical solution was worked out by Stokes. The velocity profile is sketched in Figure 3.2:2.

From the solution (15) we can obtain the *rate of flow* through the tube by an integration,

$$Q = 2\pi\int_0^a ur\,dr. \tag{16}$$

This leads to the *Poiseuille formula*,

$$Q = -\frac{\pi a^4}{8\mu}\frac{dp}{dx} = -\frac{\pi a^4}{8\mu}\frac{\Delta p}{L}. \tag{17}$$

Here, in the last term, Δp represents the pressure drop in a segment of blood vessel of length L. Δp varies linearly with L because dp/dx is a constant. Dividing the rate of flow by the cross-sectional area of the tube yields the *mean velocity of flow* in the laminar, Poiseuillean case,

$$u_m = -\frac{a^2}{8\mu}\frac{dp}{dx}. \tag{18}$$

Finally, the shear stress at the tube wall is given by $-\mu(\partial u/\partial r)$ at $r = a$. Using Eqs. (15) and (17), we obtain

$$\begin{aligned}\text{shear stress on the tube wall} &= -\frac{a}{2}\frac{dp}{dx} = -\frac{a}{2}\frac{\Delta p}{L} \\ &= \frac{4\mu}{\pi a^3}Q = 4\mu\frac{u_m}{a}.\end{aligned} \tag{19}$$

If we divide the shear stress by the mean dynamic pressure $\frac{1}{2}\rho u_m^2$ the ratio is called the *skin friction coefficient*. Denoting the skin friction coefficient by C_f, we obtain, for a laminar Poiseuillean flow,

$$C_f = \frac{\text{shear stress}}{\text{mean dynamic pressure}} = \frac{-\mu(\partial u/\partial r)_{r=a}}{\rho u_m^2} = \frac{16}{N_R}, \tag{20}$$

where N_R is the Reynolds number,

$$N_R = 2au_m/\nu. \tag{21}$$

The formula for shear stress on the wall in a laminar Poiseuillean flow is then

$$\text{shear stress} = C_f \tfrac{1}{2}\rho u_m^2. \tag{22}$$

Hagen and Poiseuille obtained Eq. (13) through experimental measurements; it was their empirical formula. The theoretical derivation was due to Stokes. Equation (13) is not valid near the entrance or exit section of a tube. It is satisfactory at a sufficiently large distance from the ends, but is again invalid if the tube is too large or if the velocity is too high. The difficulty at the entry or exit region is due to the transitional nature of the flow in that region, so that our assumption $v = 0$, $w = 0$ is not valid. The difficulty with too large a Reynolds number, however, is of a different kind: The flow becomes turbulent!

Osborne Reynolds demonstrated the transition of a laminar flow to a turbulent flow in a pipe by a classical experiment in which he examined the flow in a small outlet from a large water tank. He used a stopcock at the end of the tube to control the speed of water flow through the tube. The junction of the tube with the tank was nicely rounded, and a filament of colored fluid was introduced at the mouth. When the speed of water was slow, the filament remained distinct through the entire length of the tube. When the speed was increased, the filament broke up at a given point and diffused throughout the cross section (Fig. 3.2:3). Reynolds identified the governing parameter $u_m d/\nu$—the Reynolds number—where u_m is the mean velocity, d is the diameter, and ν is the kinematic viscosity. The region in which the colored filament diffuses to the whole tube is the transition zone from laminar to turbulent flow in the tube. Reynolds found that transition occurred at Reynolds numbers between 2,000 and 13,000, depending on the smoothness of the tube wall and the shape of the entry condition. When extreme care is taken, the transition can be delayed to Reynolds numbers as high as 40,000. On the other hand, a value of 2,000 appears to be about the lowest value obtainable on a rough entrance. This is interesting, but hard to understand. Indeed, turbulence is one of the most difficult problems in fluid mechanics.

The theoretical solution can be modified to account for the non-Newtonian rheological properties of blood, which have been discussed in Sections 3.1 and 3.2 in *Biomechanics: Mechanical Properties of Living Tissues* (Fung, 1993b). Steady flow of blood in circular cylindrical tubes is discussed in Section 3.3 of that book. It is shown that the effect of nonlin-

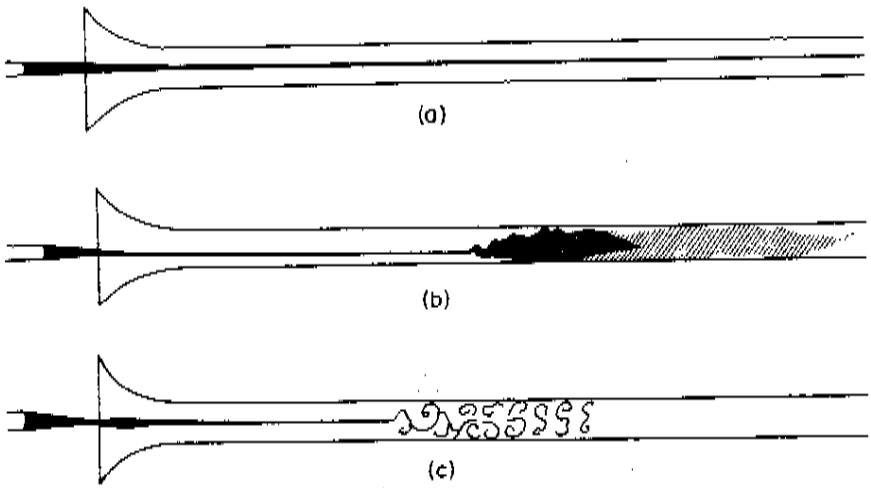

FIGURE 3.2:3. Reynolds' turbulence experiment: (a) laminar flow; (b) and (c) transition from laminar to turbulent flow. After Reynolds, O. (1883): An experimental investigation of the circumstances which determine whether the motion of water shall be direct or sinuous, and of the law of resistance in parallel channels. *Phil. Trans. Roy. Soc.* **174**: 935–982.

ear blood rheology on the resistance of blood flow in arteries is relatively minor but its effect on flow separation can be great.

Historically, the great significance of Poiseuille's contribution is at least fourfold: (a) The great precision of his results. (b) By using tubes of very small diameters, he made sure that the flow was laminar. (c) Stokes and others have regarded the agreement of Poiseuille's empirical formula with theoretical prediction based on the Navier–Stokes equation as a proof of the *no-slip condition on the solid boundary* mentioned in Section 2.6. The importance of the no-slip condition is paramount; the theoretical derivation of this condition is forever fascinating. (d) Poiseuille made this study for the explicit purpose of laying the foundation of biomechanics.

3.3 Applications of Poiseuille's Formula: Optimum Design of Blood Vessel Bifurcation

Poiseuille's formula has many uses. It tells us that the most effective factor controlling blood flow is the radius of the blood vessel. For a given pressure drop, a 1% change in vessel radius will cause a 4% change in blood flow. Conversely, if an organ needs a certain amount of blood flow to function, then the pressure difference needed to send this flow through depends on the vessel radius. For a fixed flow a 1% decrease in vessel radius will

cause a 4% increase in the required pressure difference. This is seen from Eq. (3.2:17) as follows:

a. If Δp, μ, and L are constant, then by taking the logarithm on both sides of the equation and differentiating, we obtain

$$\frac{\delta \dot{Q}}{\dot{Q}} = 4\frac{\delta a}{a}. \tag{1}$$

b. If $\dot{Q}$, μ, and L are constant, then by differentiation and rearranging terms, we obtain

$$\frac{\delta(\Delta p)}{\Delta p} = -4\frac{\delta a}{a}. \tag{2}$$

Hence an effective way of controlling blood pressure is to change the vessel radius. Hypertension (high blood pressure) can be caused by narrowing of blood vessels, and can be reduced by relaxing the smooth muscle tension that controls the blood vessel radius. Reducing blood viscosity is another way of reducing the resistance to blood flow, and hemodilution is sometimes used in surgery.

Now let us consider a different application. We know that arteries bifurcate many times before they become capillaries. Can we guess at a design principle of the blood vessel bifurcation? To be more concrete, let us consider three vessels, AB, BC, and BD, connecting three points, A, C, and D, in space (Fig. 3.3:1). There is a flow $\dot{Q}_0$ coming through A into AB. The flow is divided into $\dot{Q}_1$ in BC and $\dot{Q}_2$ in BD. Let the points A, C, D be fixed, but the location of B and the vessel radii are left for the designer to choose. Is there an optimal position for the point B?

By asking such a question we are seeking a principle of optimum design. Some *cost function* is assumed, and the design parameters are chosen so that the cost function is minimized. Some of the great theories of physics and chemistry are based on such principles. One may recall the principle

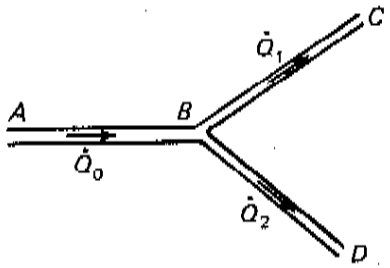

FIGURE 3.3:1. Bifurcation of a blood vessel AB into two branches BC and BD, supplying blood at a rate of $\dot{Q}_0$ (cm^3/sec) from point A to points C and D, with outflow of $\dot{Q}_1$ at C and $\dot{Q}_2$ at D.

of minimum potential energy in elasticity, the principle of minimum entropy production in irreversible thermodynamics, the Fermat principle of least time of travel in optics, Maupertius' principle of least action, Hamilton's principle in physics, and so on. The potential energy, entropy production, travel time, action, and the Hamiltonian are the cost functions in these cases.

For blood vessels, Murray (1926) and Rosen (1967) proposed a cost function that is the sum of the rate at which work is done on the blood and the rate at which energy is used up by the blood vessel by metabolism. The former is the product of $\dot{Q}\Delta p$. The latter is assumed to be proportional to the volume of the vessel $\pi a^2 L$, with a proportional constant K. Hence

$$\text{Cost function for blood vessels} = \dot{Q}\Delta p + K\pi a^2 L. \tag{3}$$

With Eq. (3.2:17) we can write

$$\text{Cost function} = \frac{8\mu L}{\pi a^4}\dot{Q}^2 + K\pi a^2 L. \tag{4}$$

The cost function of the entire system of blood vessels is the sum of the cost functions of individual vessel segments. Hence, each vessel must be optimal and the system must be put together optimally. For a given vessel of length L and flow $\dot{Q}$, there is an optimal radius a, which can be calculated by minimizing the cost function with respect to a. At the optimal condition, the following derivative must vanish:

$$\frac{\partial}{\partial a}(\text{cost function}) = -\frac{32\mu L}{\pi}\dot{Q}^2 a^{-5} + 2K\pi L a = 0. \tag{5}$$

This yields the solution

$$a = \left(\frac{16\mu}{\pi^2 K}\right)^{1/6}\dot{Q}^{1/3}. \tag{6}$$

Hence, the optimal radius of a blood vessel is proportional to $\dot{Q}$ to the 1/3 power. On substituting (6) into (4), we obtain the minimum value of the cost function:

$$\text{Min. cost function} = \frac{3\pi}{2}KLa^2. \tag{7}$$

Bifurcation Pattern

Now consider the bifurcation problem. Since the cost functions of all vessels are additive, we see at once that the vessels connecting A, C, and D in Figure 3.3:1 should be straight and lie in a plane (because this minimizes the length, L, when other things are fixed.) To find out the details let the geometric parameters be specified as shown in Figure 3.3:2. The three branches

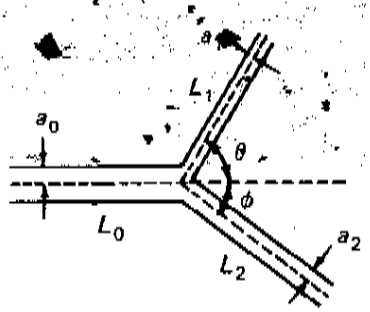

FIGURE 3.3:2. Geometric parameters of the branching pattern. Theory shows that B should lie in the plane of ACD.

will be denoted by subscripts 0, 1, 2. The total cost function will be denoted by P:

$$P = \frac{3\pi K}{2}\left(a_0^2 L_0 + a_1^2 L_1 + a_2^2 L_2\right). \tag{8}$$

The lengths L_0, L_1, L_2 are affected by the location of the point B, and the radii a_0, a_1, a_2 are related to the flows Q_0, Q_1, Q_2 through Eq. (6). Let us now minimize P by properly choosing the location of the bifurcation point B.

Since a small movement of B changes P by

$$\delta P = \frac{3\pi K}{2}\left(a_0^2 \delta L_0 + a_1^2 \delta L_1 + a_2^2 \delta L_2\right), \tag{9}$$

an optimal location of B would make $\delta P = 0$ for arbitrary small movement of B. Let us consider three special movements of B. First, let B move to B′ in the direction of AB, as shown in Figure 3.3:3. In this case

$$\delta L_0 = \delta, \quad \delta L_1 = -\delta\cos\theta, \quad \delta L_2 = -\delta\cos\phi,$$

$$\delta P = \frac{3\pi K}{2}\delta\left(a_0^2 - a_1^2\cos\theta - a_2^2\cos\phi\right). \tag{10}$$

The optimum is obtained when

$$a_0^2 = a_1^2\cos\theta + a_2^2\cos\phi. \tag{11}$$

Next, let B move to B′ in the direction of CB, as shown in Figure 3.3:4. Then

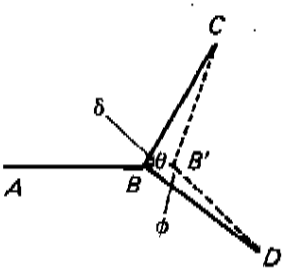

FIGURE 3.3:3. A particular variation of δL_0, δL_1, δL_2 by a small displacement of B in the direction of AB.

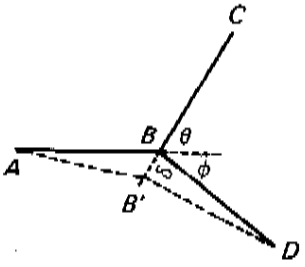

FIGURE 3.3:4. Another particular variation of δL_0, δL_1, δL_2 by a displacement of B to B' along BC.

$$\delta L_0 = -\delta\cos\theta, \quad \delta L_1 = \delta, \quad \delta L_2 = \delta\cos(\theta+\phi),$$

$$\delta P = \frac{3\pi K\delta}{2}\left[-a_0^2\cos\theta + a_1^2 + a_2^2\cos(\theta+\phi)\right], \tag{12}$$

and the optimal condition is

$$-a_0^2\cos\theta + a_1^2 + a_2^2\cos(\theta+\phi) = 0. \tag{13}$$

Finally, let B move a short distance δ in the direction of DB (Fig. 3.3:5). Then the optimal condition is obviously,

$$-a_0^2\cos\phi + a_1^2\cos(\theta+\phi) + a_2^2 = 0. \tag{14}$$

Solving Eqs. (11), (13), and (14) for $\cos\theta$, $\cos\phi$, and $\cos(\theta+\phi)$, we obtain

$$\cos\theta = \frac{a_0^4 + a_1^4 - a_2^4}{2a_0^2a_1^2},$$

$$\cos\phi = \frac{a_0^4 - a_1^4 + a_2^4}{2a_0^2a_2^2},$$

$$\cos(\theta+\phi) = \frac{a_0^4 - a_1^4 - a_2^4}{2a_1^2a_2^2}. \tag{15}$$

The equation of continuity (conservation of mass) is

$$Q_0 = Q_1 + Q_2. \tag{16}$$

By Eq. (6), this is

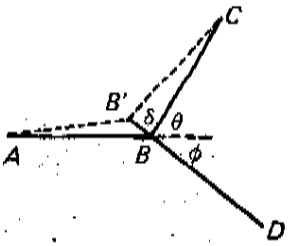

FIGURE. 3.3:5. A third variation caused by a displacement of B to B' along BD.

$$a_0^3 = a_1^3 + a_2^3, \tag{17}$$

which is often referred to as Murray's law. Thus Eq. (15) can be reduced to

$$\cos\theta = \frac{a_0^4 + a_1^4 - \left(a_0^3 - a_1^3\right)^{4/3}}{2a_0^2 a_1^2}, \quad \text{etc.} \tag{18}$$

Ghassan Kassab has collected an extensive set of data on the coronary arteries of the pig (see Chapter 7; Kassab et al., 1993), and Kassab and Fung (1995) tested Murray's law, Eq. (17), against the experimental data. They found excellent agreement of Murray's law and experimental data from control and hypertensive hearts. Oka (1974) has proposed to improve Murray's cost function by adding a term of metabolic cost proportional to the volume of the blood vessel wall. Oka's cost function is a modification of Eq. (4):

$$\text{Cost } P = \frac{8\mu L}{\pi a^4}\dot{Q}^2 + K\pi a^2 L + K_w 2\pi a h L \tag{19}$$

where K_w and h are the metabolic constant and thickness of the vessel wall, respectively, and are assumed to be constant. Kassab and Fung (1995) found Oka's modified Murray's law does not improve the agreement.

Applications of these formulas are illustrated in the following Problems.

Problems

3.1 Show that, according to Murray's cost function, if $a_1 = a_2$, then $\theta = \phi$. Thus, if the radii of the daughter branches are equal, the bifuracting angles are equal.

3.2 Show that if $a_2 > a_1$, then $\theta > \phi$.

3.3 Show that if $a_2 \gg a_1$, then $a_2 \doteq a_0$ and $\phi \doteq \pi/2$.

3.4 When $a_1 = a_2$, show that $a_1/a_0 = 2^{-1/3} = 0.794$, and $\cos\theta = 0.794$. Thus $\theta \doteq 37.5°$.

3.5 The cost function specified in Eq. (4) is somewhat arbitrary. Develop some other cost functions and deduce the consequences, such as

(a) Minimum total surface area of the blood vessels,
(b) Minimum total volume of the blood vessels,
(c) Minimum power for the blood flow,
(d) Minimum total shear force on the vessel wall.

See Kamiya and Togawa (1972), Murray (1926), and Zamir (1976, 1977).

The results of Problems 3.1–3.4 are in reasonable agreement with empirical observations. The result of Problem 3.4 is especially interesting.

Let a_0 denote the radius of the aorta, and assume equal bifurcation in all generations. Then the radius of the first generation is $0.794\ a_0$, that of the second generation is $(0.794)^2\ a_0$, and, generally, that of the nth generation is

$$a_n = (0.794)^n a_0 \tag{20}$$

If a capillary blood vessel has a radius of 5×10^{-4} cm and the radius of the aorta is $a_0 = 1.5$ cm, then Eq. (20) yields $n \doteq 30$. Thus 30 generations of equal bifurcation are needed to reduce that aorta to the capillary dimension. Since each generation multiplies the number of vessels by 2, the total number of blood vessels is $2^{30} \doteq 10^9$. But these estimates cannot be taken too seriously, because arteries rarely bifurcate symmetrically (as required by the hypothesis $a_1 = a_2$). There is one symmetric bifurcation of the arteries of humans; there is none in the dog.

The Uniform Shear Hypothesis

Problem 3.5 is very significant. It turns out that several cost functions lead to almost the same results. Zamir (1976) deduced that the shear stress on blood vessel wall is uniform throughout the arterial system according to his principle of minimum total shear force. The hypothesis of uniform shear stress or shear strain gradient and constant coefficient of viscosity on the blood vessel wall has been supported by several studies. Kamiya and Togawa (1980) surgically constructed an arteriovenous shunt from the common carotid artery to the external jugular vein, causing an increase of blood flow in one segment of the artery and a decrease of flow in another. They then showed that 6 to 8 months after the operation, the segment with increased flow dilated, while the segment with decreased flow atrophied to a smaller diameter, just enough so that the shear strain rate remained almost constant if the change of flow was within four times of the control. Liebow (1963), Thoma (1893) and others, on observing embryologic vascular development and studying arteriovenous fistulas and collateral circulation, have shown that increased flow induces vessel growth, reduced flow leads to atrophy. Rodbard (1975) collected clinical evidence of the same. Then Friedman and Deters (1987), Giddens et al. (1990), and Kamiya et al, (1984) collected data from literature and their own research and concluded that the arterial wall shear stress on dog's peripheral and coronary arterioles, arteries, and aorta lies in a remarkably narrow range of 10–20 dynes/cm^2.

Kassab and Fung (1995) showed that if the Poiseuille formula given in Eq. (19) of Section 3.2 is substituted into the equation of continuity Eq. (16), one obtains the relation

$$\left(a_0^3/\mu_0\right)\tau_{w0} = \left(a_1^3/\mu_1\right)\tau_{w1} + \left(a_2^3/\mu_2\right)\tau_{w2} \tag{21}$$

or

$$a_0^3\gamma_0 = a_1^3\gamma_1 + a_2^3\gamma_2 \tag{22}$$

Where τ_w denotes shear stress and γ denotes shear strain rate, $\gamma = \partial u/\partial y$, on the blood vessel wall, with γ_0, γ_1, γ_2, τ_{w0}, τ_{w1}, τ_{w2}, and μ_0, μ_1, μ_2 refer to the values of γ, τ_w, and μ at the boundaries of the tubes 0, 1, 2, respectively. Now, if one introduces the hypothesis that the shear strain rate or the coefficients of viscosity and the wall shear stresses are the same in all three vessels, then Eqs. (21) and (22) become Murray's law, Eq. (17). On the other hand, if we assume Murray's law as an empirical fact, then the coexistence of Eqs. (17), (21) and (22) implies that

$$\tau_{w0} = \tau_{w1} = \tau_{w2}, \quad \gamma_0 = \gamma_1 = \gamma_2 \tag{23}$$

Thus, Murray's law and Poiseuille's law imply uniform shear; and vice versa, uniform shear and Poiseuille's law imply Murray's law.

Finally, the rate of viscous dissipation per unit volume of blood is equal to the product of shear stress and strain rate. At the blood vessel wall, this is:

$$\text{Volumetric rate of viscous dissipation} = \tau_w\gamma_w. \tag{24}$$

Thus the uniformity of shear implies a uniform energy dissipation throughout the arteriolar walls.

Stress Distribution on Blood Vessel Wall and in Endothelial Cells

The wall shear stress discussed in Poiseuille flow is defined at the length scale hierarchy level of the blood vessel diameter. If we go one level lower, to the scale of a single endothelial cell, a very different picture exists. At level, the endothelium surface is wavy, with hills and valleys. The no-slip condition must be applied on the cell membranes facing the blood. The hills and valleys will cause nonuniform shear stress distribution, even if the shear flow far above the surface is uniform. Inside the individual endothelial cells, there is another world of structures and materials. Intracellular mechanics must be investigated at smaller and smaller scales. Finally, there is also a class of problems concerned with the long-range variation of certain features in individual cells. An example is the longitudinal variation of tensile and shear stresses in the endothelial cell membranes along the length of the aorta, as discussed by Fung and Liu (1993) and Liu et al. (1994).

3.4 Steady Laminar Flow in an Elastic Tube

As another application of Poiseuille's formula, let us consider the flow in a circular cylindrical elastic tube (Fig. 3.4:1). The flow is maintained by a pressure gradient. The pressure in the tube is, therefore, nonuniform—higher at

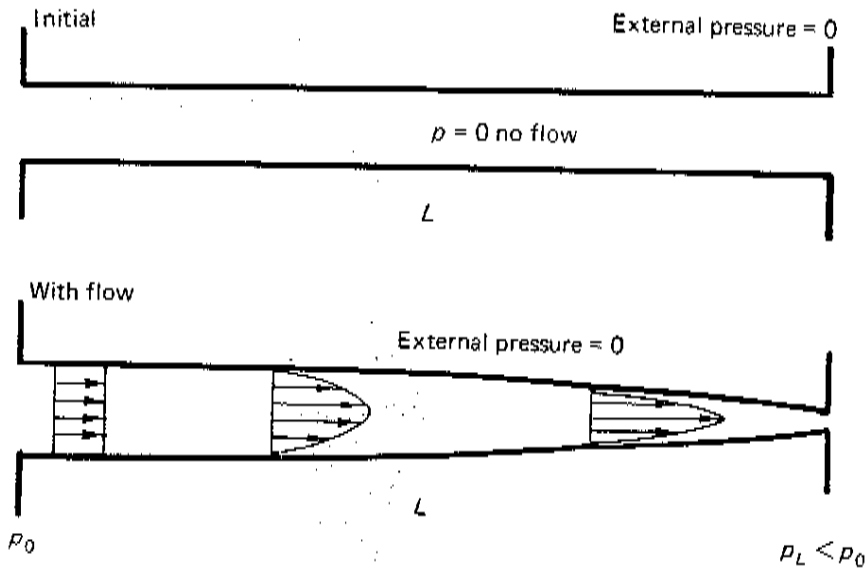

FIGURE 3.4:1. Flow in an elastic tube of length L.

the entry end and lower at the exit end. Because the tube is elastic, the high-pressure end distends more than the low-pressure end. The diameter of the tube is, therefore, nonuniform (if it were uniform originally), and the degree of nonuniformity depends on the flow rate.

If we wish to determine the pressure–flow relationship for such a system, we may break down the problem into two familiar components. This is illustrated in Figure 3.4:2. In the lower block, we regard the vessel as a rigid conduit with a specified wall shape. For a given flow, we compute the pressure distribution. This pressure distribution is then applied as loading on the elastic tube, represented by the upper block. We then analyze the deformation of the elastic tube in the usual manner of the theory of elasticity. The result of the calculation is then used to determine the boundary shape of the hydrodynamic problem of the lower block. Thus, back and forth, until a consistent solution is obtained, the pressure distribution corresponding to a given flow is determined.

Let us put this in mathematical form. Assume that the tube is long and slender, that the flow is laminar and steady, that the disturbances due to entry and exit are negligible, and that the deformed tube remains smooth and slender. These assumptions permit us to consider the solution given in Section 3.2 as valid (a good approximation) everywhere in the tube. Assuming a Newtonian fluid, we have (Eq. (17) of Sec. 3.2)

$$\frac{dp}{dx} = -\frac{8\mu}{\pi a^4} Q \tag{1}$$

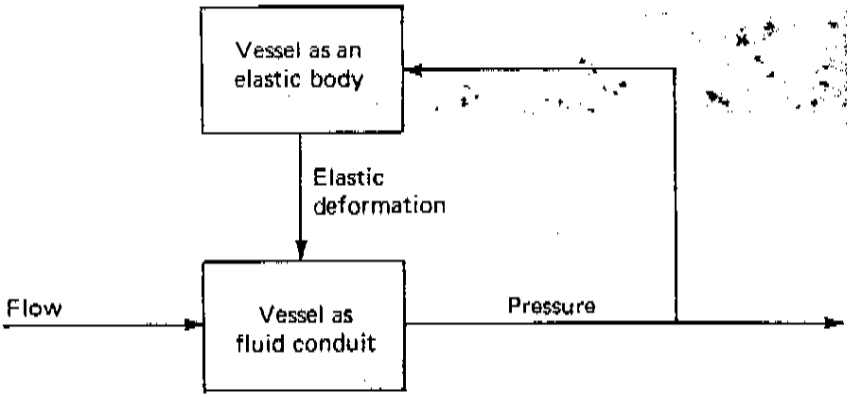

FIGURE 3.4:2. A hemoelastic system analyzed as a feedback system of two functional units: an elastic body and a fluid mechanism.

Here $\dot{Q}$ is the volume–flow rate. In a stationary, nonpermeable tube $\dot{Q}$ is a constant throughout the length of the tube. The tube radius is a, which is a function of x because of the elastic deformation. An integration of Eq. (1) yields

$$p(x) = p(0) - \frac{8\mu}{\pi}\dot{Q}\int_0^x \frac{1}{[a(x)]^4}\,dx. \tag{2}$$

The integration constant is $p(0)$, the pressure at $x = 0$. The exit pressure is given by Eq. (2) with $x = L$. L is the length of the tube.

Now let us turn our attention to the calculation of the radius $a(x)$. Let the tube be initially straight and uniform, with a radius a_0. Assume that the tube is thin walled, and that the external pressure is zero (Fig. 3.4:3). (If the external pressure was not zero, we would replace p in Eq. (3) by the difference of internal and external pressures.) Then a simple analysis yields the average circumferential stress in the wall:

$$\sigma_{\theta\theta} = \frac{p(x)a(x)}{h}, \tag{3}$$

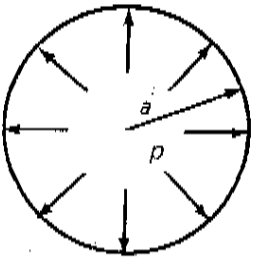

FIGURE 3.4:3. Distension of an elastic tube due to internal pressure.

where h is the wall thickness (Fung, 1993a, p. 25). Let the axial length and tension be constant, and assume that the material obeys Hooke's law. Then the circumferential strain is

$$e_{\theta\theta} = \frac{\sigma_{\theta\theta}}{E}, \tag{4}$$

where E is the Young's modulus of the wall material. (Srictly, the right-hand side of Eq. (4) should be

$$\frac{1}{E}\left(\sigma_{\theta\theta} - \nu\sigma_{rr}\right),$$

where ν is the Poisson's ratio. But σ_{rr} is, in general, much smaller than $\sigma_{\theta\theta}$ for thin-walled tubes.) The strain $e_{\theta\theta}$ is equal to the change of radius divided by the original radius, a_0:

$$e_{\theta\theta} = \frac{a(x) - a_0}{a_0} = \frac{a(x)}{a_0} - 1. \tag{5}$$

Combining (5), (4), and (3), we obtain

$$a(x) = a_0\left[1 - \frac{a_0}{Eh}p(x)\right]^{-1}. \tag{6}$$

Substituting (6) into (1), we may write the result as

$$\left(1 - \frac{a_0}{Eh}p\right)^{-4} dp = -\frac{8\mu}{\pi a_0^4} Q dx. \tag{7}$$

Recognizing the boundary conditions $p = p(0)$ when $x = 0$ and $p = p(L)$ when $x = L$, and integrating Eq. (7) from $p(0)$ to $p(L)$ on the left and 0 to L on the right, we obtain the pressure–flow relationship:

$$\frac{Eh}{3a_0}\left\{\left[1 - \frac{a_0}{Eh}p(L)\right]^{-3} - \left[1 - \frac{a_0}{Eh}p(0)\right]^{-3}\right\} = -\frac{8\mu}{\pi a_0^4} LQ, \tag{8}$$

which shows that the flow is not a linear function of pressure drop $p(0) - p(L)$.

Another Solution

The solution obtained in Eq. (8) is based on the assumption of Hooke's law. Most blood vessels do not obey Hooke's law, their zero-stress states are open sectors, and their constitutive equations are nonlinear (see Section 2.6, pp. 56–60, and Section 3.8, p. 145).

A simple result can be obtained if we assume the pressure–radius relationship to be linear:

$$a = a_0 + \alpha p/2. \tag{9}$$

Here a_0 is the tube radius when the transmural pressure is zero. α is a compliance constant. Equation (9) is a good representation of the pulmonary blood vessels (see Sec. 4.10, Fig. 4.10:2, p. 257 and Sec. 6.7, Fig. 6.7:4).

Using Eq. (9), we have

$$\frac{dp}{dx} = \frac{dp}{da}\frac{da}{dx} = \frac{2}{\alpha}\frac{da}{dx}. \tag{10}$$

On substituting Eq. (10) into Eq. (1) and rearranging terms, we obtain

$$a^4 \frac{da}{dx} = \frac{1}{5}\frac{da^5}{dx} = -\frac{4\mu\alpha}{\pi}\dot{Q}. \tag{11}$$

Since the right-hand side term is a constant independent of x, we obtain at once the integrated result

$$\left[a(x)\right]^5 = -\frac{20\mu\alpha}{\pi}\dot{Q}x + \text{const}. \tag{12}$$

The integration constant can be determined by the boundary condition that when $x = 0$, $a(x) = a(0)$. Hence the constant $= [a(0)]^5$. Then, by putting $x = L$, we obtain from Eq. (12) the elegant result

$$\frac{20\mu\alpha L}{\pi}\dot{Q} = \left[a(0)\right]^5 - \left[a(L)\right]^5. \tag{13}$$

The pressure–flow relationship is obtained by substituting Eq. (9) into Eq. (13). Thus the flow varies with the difference of the fifth power of the tube radius at the entry section ($x = 0$) minus that at the exit section ($x = L$). If the ratio $a(L)/a(0)$ is 1/2, then $[a(L)]^5$ is only about 3% of $[a(0)]^5$, and is negligible by comparison. Hence when $a(L)$ is one half of $a(0)$ or smaller, the flow varies directly with the fifth power of the tube radius at the entry, whereas the radius (and the pressure) at the exit section has little effect on the flow.

Problems

3.6 If the elastic deformation is small,

$$\frac{a_0 p(0)}{Eh} \ll 1, \quad \frac{a_0 p(L)}{Eh} \ll 1,$$

show that the pressure–flow relationship Eq. (8) or (13) then becomes approximately linear.

3.7 Plot curves to show the flow–pressure relationship given by Eqs. (8) and (13), and discuss the results.

3.8 The actual relationship between the pressure and radius in peripheral blood vessels is nonlinear. See Chapter 8 of *Biomechanics: Mechanical*

Properties of Living Tissues (Fung, 1993b). Outline a theory that will take into account the nonlinear pseudo-elastic stress–strain relationship in deriving the pressure–flow relationship of the blood vessel.

3.9 Outline further a theory that will take into account the viscoelastic behavior of the blood vessel in deriving the pressure–flow relationship of the blood vessel.

3.5 Dynamic Similarity. Reynolds and Womersley Numbers. Boundary Layers

Consider first a blood flow in which the shear rate is sufficiently high so that the blood has a constant coefficient of viscosity. Then the Navier–Stokes equations presented in Section 2.6 apply. This equation is

$$\rho\frac{\partial u_i}{\partial t}+\rho\left(u_1\frac{\partial u_i}{\partial x_1}+u_2\frac{\partial u_i}{\partial x_2}+u_3\frac{\partial u_i}{\partial x_3}\right)$$
$$=X_i-\frac{\partial p}{\partial x_i}+\mu\left(\frac{\partial^2}{\partial x_1^2}+\frac{\partial^2}{\partial x_2^2}+\frac{\partial^2}{\partial x_3^2}\right)u_i. \tag{1}$$

Here u_i denotes the velocity vector, with the index i ranging over 1, 2, 3, so that the components of u_i are u_1, u_2, u_3, or u, v, w, x_i, with components x_1, x_2, x_3 or x, y, z, is a position vector referred to a rectangular cartesian frame of reference. ρ is the density or mass per unit volume of the fluid. X_i is the body force per unit volume. p is pressure. μ is the coefficient of viscosity of the fluid. μ/ρ is called *kinematic viscosity*, and is designated by a Greek symbol ν which will be used later.

Equation (1) represents the balance of four kinds of forces. Term by term, they are

transient inertia force per unit vol	+	convective inertia force per unit vol	=	body force per unit vol	+	pressure force on sides of unit control vol	+	viscous force on sides of unit control vol

Let us put the Navier–Stokes equation in dimensionless form. Choose a characteristic velocity V, a characteristic frequency ω and a characteristic length L. For example, if we investigate the flow in the aorta, we may take V to be the average speed of flow, ω to be the heart rate, and L to be the blood vessel diameter. Having chosen these characteristic quantitites, we introduce the dimensionless variables

$$x' = \frac{x}{L}, \quad y' = \frac{y}{L}, \quad z' = \frac{z}{L}, \quad u' = \frac{u}{V},$$
$$v' = \frac{v}{V}, \quad w' = \frac{w}{V}, \quad p' = \frac{p}{\rho V^2}, \quad t' = \omega t, \tag{2}$$

and the parameters

$$\text{Reynolds number} = N_R = \frac{VL\rho}{\mu} = \frac{VL}{\nu}, \tag{3}$$

$$\text{Stokes number} = N_S = \frac{\omega L^2}{\nu}, \tag{4}$$

$$\text{Womersley number } \alpha = N_w = \sqrt{N_S} = L\sqrt{\left(\frac{\omega}{\nu}\right)}. \tag{5}$$

On substituting Eqs. (2) to (5) into Eq. (1), omitting body force, and dividing through by $\rho V^2/L$, we obtain

$$\frac{N_S}{N_R}\frac{\partial u'}{\partial t'} + u'\frac{\partial u'}{\partial x'} + v'\frac{\partial u'}{\partial y'} + w'\frac{\partial u'}{\partial z'} = -\frac{\partial p'}{\partial x'} + \frac{1}{N_R}\left(\frac{\partial^2 u'}{\partial x'^2} + \frac{\partial^2 u'}{\partial y'^2} + \frac{\partial^2 u'}{\partial z'^2}\right) \tag{6}$$

and two additional equations obtainable from Eq. (6) by changing u' into v', v' into w', w' into u' and x' into y', y' into z', z' into x'. The body force is ignored. The $\partial\mu/\partial x_k$ term is dropped because μ is a constant. The equation of continuity (Eq. 8 of Sec. 2.6) can also be put in dimensionless form:

$$\frac{\partial u'}{\partial x'} + \frac{\partial v'}{\partial y'} + \frac{\partial w'}{\partial z'} = 0. \tag{7}$$

Since Eqs. (6) and (7) constitute the complete set of field equations for an incompressible fluid, it is clear that only two physical parameters, the Reynolds number N_R, and the Womersley number N_w, enters into the field equations of the flow.

To solve these equations for a specific problem we must consider the boundary equations. Consider two flows in two geometrically similar vessels. The vessels have the same shape but different sizes. The boundary conditions are identical (no-slip). Then the two flows will be identical (in the dimensionless variables) if the Reynolds numbers and the Womersley numbers for the two flows are the same, because two geometrically similar bodies having the same Reynolds number and Womersley number will be governed by identical differential equations and boundary conditions (in dimensionless form). Therefore, flows about geometrically similar bodies at the same Reynolds and Womersley numbers are completely similar in the sense that the functions $u'(x', y', z', t')$, $v'(x', y', z', t')$, $w'(x', y', z', t')$, $p'(x', y', z', t')$ are the same for the various flows. Thus the Reynolds and Womersley numbers are said to govern the dynamic similarity.

The Reynolds number expresses the ratio of the convective inertia force to the shear force. In a flow the inertial force due to convective acceleration arises from terms such as $\rho u \partial u/\partial x$, whereas the shear force arises from terms such as $\mu \partial^2 u/\partial y^2$. The orders of magnitude of these terms are, respectively,

$$\text{Convective inertia force: } \rho V^2/L$$
$$\text{Shear force: } \mu V/L^2$$

The ratio is

$$\frac{\text{Convective inertia force}}{\text{Shear force}} = \frac{\rho V^2/L}{\mu V/L^2} = \frac{\rho VL}{\mu} = \text{Reynolds number.} \quad (8)$$

A large Reynolds number signals a preponderant convective inertia effect. A small Reynolds number signals a predominant shear effect.

Similarly, the Womersley number expresses the ratio of the transient or oscillatory inertia force to the shear force. The transient inertia force is given by the first term of Eq. (1). If the frequency of oscillation is ω and the amplitude of velocity is V, the order of magnitude of the first term of Eq. (1) is $\rho \omega V$. The order of magnitude of the last term of Eq. (1) is, as before, $\mu V/L^2$. Thus

$$\text{Transient inertia force: } \rho \omega V$$
$$\text{Shear force: } \mu V/L^2 .$$

The ratio is

$$\frac{\text{Transient inertia force}}{\text{Shear force}} = \frac{\rho \omega L^2}{\mu} = \frac{\omega L^2}{\nu} = \text{Stokes number}$$
$$= \left(\text{Womersley Number}\right)^2. \quad (9)$$

If the Womersley number is large, the oscillatory inertia force dominates. If N_W is small, the viscous force dominates. Typical values of Reynolds and Womersley numbers in blood vessels at normal heart rate are given in Table 3.1:1, p. 110. The Womersley number is usually denoted by α.

Boundary Layers and Their Thicknesses

The concept of boundary layer was presented by Ludwig Prandtl (1875–1953) in a brief but truly epoch-making paper (1904). It can be understood by comparing the significance of various terms of the governing equation, Eq. (1). If the coefficient of viscosity of the fluid is zero, $\mu = 0$, then the fluid is said to be *ideal*, and the last term of Eq. (1) vanishes. At the solid wall, an ideal fluid must not penetrate the solid, but its tangential velocity is unrestricted. For a viscous fluid, however, the no-slip condition must

apply, no matter how small the viscosity is. Prandtl's idea is that for a fluid with small μ the influence of the no-slip condition and the last term in Eq. (1) is limited to a thin layer next to the solid wall, whereas in the bulk of the fluid the influence of no-slip is small and the last term in Eq. (1) can be dropped. If this was true, then the thickness of the boundary layer, denoted by δ, can be estimated by comparing proper terms in Eq. (1). Consider first an oscillatory velocity field of frequency ω and amplitude U. The first term of Eq. (1) shows that the transient inertia force is of the order of magnitude $\rho\omega U$. The last term in Eq. (1) shows that the order of magnitude of the viscous force is of the order of $\mu U/\delta_1^2$, where a subscript 1 is added to indicate that this boundary layer is associated with the transient acceleration. In the transient boundary layer, these two terms are of equal importance. Hence,

$$\rho\omega U = \frac{\mu U}{\delta_1^2} \tag{10}$$

or

$$\delta_1 = \sqrt{\frac{\mu}{\rho\omega}} = \sqrt{\frac{\nu}{\omega}}. \tag{11}$$

In a tube flow, let the characteristic length be the radius, L. Then the ratio of L to δ_1 is

$$\frac{L}{\delta_1} = L\sqrt{\frac{\omega}{\nu}} = \sqrt{N_S} = N_W \tag{12}$$

Hence, if the Womersley number N_W or Stokes number N_S is large, the transient boundary layer is very thin compared with the tube radius.

Next, consider the convective inertia force given by the second group of terms in Eq. (1). At a convective boundary layer thickness δ_2, the order of magnitude of the second term is $\rho U^2/L$, whereas that of the viscous force term is $\mu U^2/\delta_2^2$. In the convective boundary layer these two terms are equally important. Hence,

$$\rho U^2/L = \mu U^2/\delta_2^2 \tag{13}$$

or

$$\delta_2 = \sqrt{\frac{\mu L}{\rho U}} \tag{14}$$

The ratio of L to δ_2 is

$$\frac{L}{\delta_2} = \sqrt{\frac{\rho U L}{\mu}} = \sqrt{N_R} \tag{15}$$

i.e., the square root of the Reynolds number. Hence, when the Reynolds number is large, the convective boundary layer is very thin. In a tube flow,

at a distance from the wall much larger than δ_1 and δ_2, the fluid may be regarded as ideal.

These estimates have many applications in the following sections. In Section 3.18, it is shown that the boundary layer thickness increases with the distance from the entrance section; and there are interactions between the transient and convective boundary layers. Exact calculations can be found in Schlichting (1968).

3.6 Turbulent Flow in a Tube

In Section 3.2 we mentioned that when the Reynolds number exceeds a certain critical value the flow becomes turbulent. Turbulence is marked by random fluctuations. With turbulence the velocity field can no longer be predicted with absolute precision, but its statistical features (mean velocity, root mean square velocity, mean pressure gradient, etc.) are perfectly well defined. If a steady flow in a straight, long pipe changes from laminar to turbulent, two important changes will occur: (a) The profile of the mean velocity will become much more blunt at the center of the pipe, and (b) the shear gradient will become much greater at the wall. This is shown in Figure 1.4:1, p. 7. As a consequence of this change of velocity profile, the resistance to flow is greatly increased.

The best way to see how the resistance to flow changes with turbulence is to study the *friction coefficient*, C_f, defined in Eq. (3.2:21):

$$\text{Shear stress on pipe wall} = C_f\left(\tfrac{1}{2}\rho U_m^2\right). \tag{1}$$

Here ρ is the fluid density, U_m is the mean velocity over the cross section of the tube, capitalized here to show that this velocity is not only averaged over space, but also over a sufficiently long period of time so that the random fluctuations of turbulence are averaged out. C_f is a function of the Reynolds number (based on tube radius and the mean velocity of flow, U_m) and the roughness of the tube surface. Roughness influences the position of transition in the entrance zone of a flow into a pipe at which the flow in the boundary layer is changed from laminar to turbulent. It affects also the skin-friction drag on that portion of the surface over which the layer is turbulent.

The experimental results of Nikuradse are shown in Figure 3.6:1. The surface of the tube was sprinkled with sand of various grain sizes, which were expressed in the ratio a/ε in the figure, where a is the radius of the tube and ε is the mesh size of the screen through which the sand will just pass. The dashed straight line on the left refers to a fully developed laminar flow [Eq. (3.2:19)],

$$C_f = 16\left(\frac{2aU_m}{\nu}\right)^{-1} = \frac{16}{N_R}, \tag{2}$$

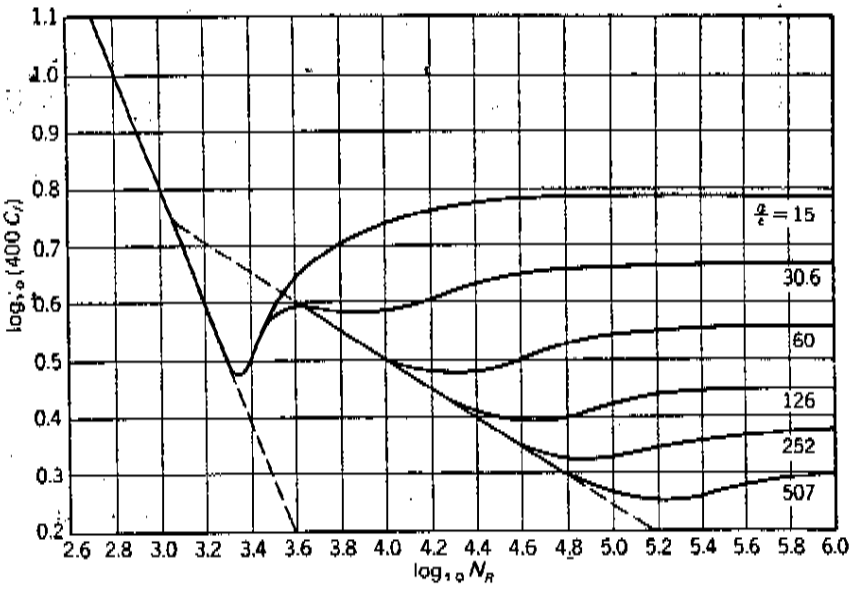

FIGURE 3.6:1. Resistance coefficient for fully developed flow through a tube of radius a with various sizes of roughness elements on the wall. ε is roughly the diameter of sand grain sprinkled on the wall. The solid curves represent the average experimental results by Nikuradse. The dashed line on the left represents a theoretical result for laminar flow. The dashed line on the right is the Blasius empirical formula for turbulent flow in a smooth tube. Based on Nikuradse, J. (1933) *Strömungsgesetze in Rauhen Rohren*, Forschungsheft 361, Ver. deutsch. Ing.

where N_R is the Reynolds number based on tube diameter and mean speed of flow. The dashed line on the right is an empirical formula given by Blasius for turbulent flow in smooth pipes,

$$C_f = 0.0655\left(\frac{U_m a}{\nu}\right)^{-1/4} = \frac{0.0779}{\left(N_R\right)^{1/4}}. \tag{3}$$

The solid curves represent the mean experimental results. It is clear that at large Reynolds numbers the friction coefficient of turbulent flow is much greater than that of laminar flow. For example, at a Reynolds number of 4,000 (i.e., $\log_{10} N_R \doteq 3.6$), a rough pipe with $a/\varepsilon = 30$ will have a skin friction about the same as that in a smooth pipe if the flow were turbulent, but it would be 2.51 times larger than that of a laminar flow if laminar flow were possible. At $N_R = 10^5$ the skin friction of a smooth pipe with turbulent flow would be 27 times larger than that given by Eq. (2), and for a rough pipe with $a/\varepsilon = 30$ the skin friction would be increased again 2.77-fold.

It seems natural to expect that natural selection in the animal world would favor laminar flow in the blood vessels so that energy is not wasted

in turbulence. Furthermore, turbulence is implicated in atherogenesis. To avoid turbulent flow in aorta, the Reynolds number should be kept below a certain critical value. Let the cardiac output (volume flow per unit time) be Q, and the radius of the aorta be R_a. Then the cross-sectional area of the aorta is πR_a^2, and the mean velocity of flow is

$$U_m = \frac{Q}{\pi R_a^2}. \tag{4}$$

The Reynolds number is

$$N_R = \frac{2U_m R_a}{\nu} = \frac{2Q}{\pi \nu R_a}. \tag{5}$$

Rosen (1967) plotted the radius of the aorta of animals versus the cardiac output, and obtained a regression line

$$R_a = 0.013Q \tag{6}$$

On substituting R_a from Eq. (6) into Eq. (5), we obtain a Reynolds number $2/(0.013\pi\nu)$, which is 1224 if $\nu = 0.04$ and 1632 if $\nu = 0.03$. These values are fairly close to but somewhat lower than the transition Reynolds number in steady flow, which seems to mean that animal aortas are designed for laminar flow, but are fairly close to the borderline of transition to turbulence.

So far our discussion of turbulence is based on steady mean flow. Pulsatile flow makes the phenomenon of laminar–turbulence transition much more complex, as is shown presently.

3.7 Turbulence in Pulsatile Blood Flow

Reynolds' experiment (see Fig. 3.2:3) shows that in pipe flow the entry region remains laminar even though turbulence develops downstream when the Reynolds number exceeds the critical value. This shows that turbulence must develop gradually in a laminar flow. It takes time for some unstable modes of motion in a flow to grow into turbulence. We may apply this concept to the pulsatile blood flow in the arteries. The flow velocity changes with time. The Reynolds number, $2aU/\nu$, based on the instantaneous velocity of flow averaged over the cross section, varies with time. Figure 3.7:1 shows a record of velocity of flow versus time. In a period of rising velocity the Reynolds number increases slowly until it reaches a level marked by the dotted line ($N_R = 2{,}300$), at which the flow could be expected to become turbulent if it were steady. But an accelerating flow is more stable than a steady flow, because turbulence cannot develop instantaneously. So, when the turbulence finally sets in, the velocity and N_R are much higher than the dotted line level. On the other hand, in a

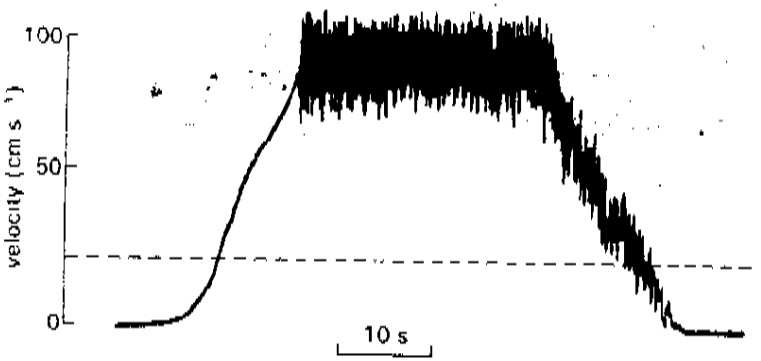

FIGURE 3.7:1. A turbulent flow velocity-versus-time record made with a hot-film probe in a pipe in which the flow rate was slowly increased until turbulence occurred, and later stopped. Peak Reynolds number was 9,500. The dotted line corresponds to Reynolds number 2,300. From Nerem, R., and Seed, W.A. (1972) An in vivo study of aortic flow disturbances, *Cardiovasc. Res.* 6: 1–14, by permission.

period of decreasing velocity the disappearance of turbulence occurs at a level of velocity considerably below the dotted line. This is partly because decelerating flow is inherently less stable than steady flow, and partly because existing eddies take a finite time to decay. Thus, the *critical Reynolds number* of laminar–turbulent transition depends on the rate of change of velocity, as well as on the eddies upstream and the roughness of the pipe wall.

The experiment corresponding to Figure 3.7:1 was designed to show the transition from laminar to turbulent flow and vice versa. Figure 3.7:2 shows a record of velocity waves from the upper descending aorta of an anesthetized dog. Turbulence is seen during the deceleration of systolic flow. Hot-film anemometry was used to obtain such records.

Quantitative studies of the laminar–turbulent transition may seek to express the critical Reynolds number as a function of the Womersley number. Experimental results are plotted in Figure 3.7:3. The ordinate is the peak Reynolds number. The stippled area indicates the conditions under which the flow is stable and laminar. In the experiments, the wide variations of velocity and heart rate were obtained with drugs and nervous stimuli in anesthetized dogs. In normal, conscious, free-ranging dogs the peak Reynolds number usually lies in an area high above the stippled area of Figure 3.7:3. This suggests that some turbulence is generally tolerated in deceleration of systolic flow in the dog.

Turbulence in blood flow implies a fluctuating pressure acting on the arterial wall and an increased shear stress. These stresses are implicated in murmurs, poststenotic dilatation, and atherogenesis. Experimental methods are described in Deshpande and Giddens (1980), and Nerem et al. (1972).

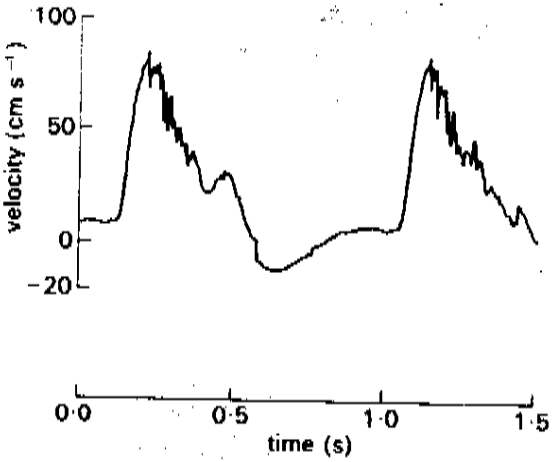

FIGURE 3.7:2. A record of velocity-versus-time of blood flow in the upper descending aorta of a dog, showing turbulence during the deceleration of systolic flow. From Seed, W.A., and Wood, N.B. (1971) Velocity patterns in the aorta. *Cardiovasc. Res.*, **5**: 319–333, by permission.

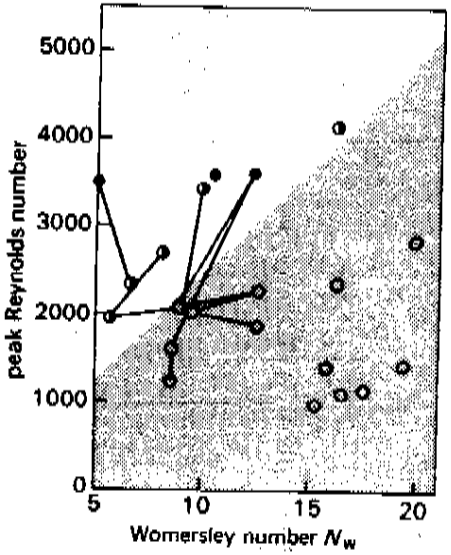

FIGURE 3.7:3. The stability of blood flow in the descending aorta of anesthetized dogs as influenced by the peak Reynolds number and the Womersley number. Points joined by the lines refer to the same animal. Open circles, laminar flow; filled circles, turbulent flow; half-filled circles, transiently turbulent flow. From Nerem, R.M., and Seed, W.A. (1972) An in vivo study of aortic flow disturbances. *Cardiovasc. Res.* **6**: 1–14, by permission.

For pulsatile flow in a tube, when the Womersley number is large, the effect of the viscosity of the fluid does not propagate very far from the wall. In the central portion of the tube the transient flow is determined by the balance of the inertial forces and pressure forces as if the fluid were non-viscous. We therefore expect that when the Womersley number is large the velocity profile in a pulsatile flow will be relatively blunt, in contrast to the parabolic profile of the Poiseuillean flow, which is determined by the balance of viscous and pressure forces. That this is indeed the case can be seen from Figures 3.7:4 and 3.7:5. In Figure 3.7:4 the velocity profiles constructed from time-mean measurements at several sites along the aorta of the dog are shown. They are seen to be quite blunt in the central portion of the aorta. Similar profiles constructed from instantaneous measurements show that this is true throughout the flow cycle.

Figure 3.7:5 shows the theoretical velocity profiles computed for a straight circular cylindrical tube in which a sinusoidally oscillating pressure gradient acts. As the Womersley number increases from 3.34 to 6.67, the

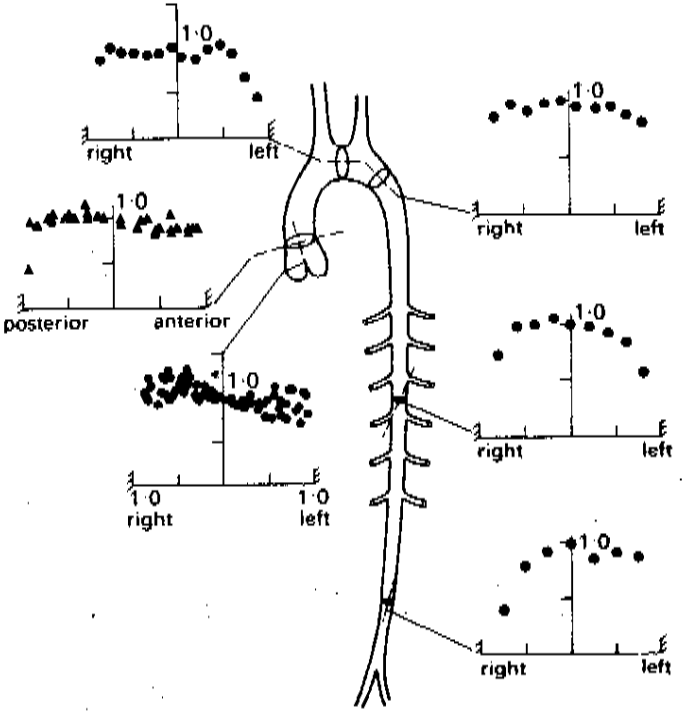

FIGURE 3.7:4. Normalized mean velocity profiles in dog aorta. The mean velocity at each site is normalized by dividing through by the centerline mean velocity. From Schultz, D.L. (1972) Pressure and flow in large arteries. In *Cardiovascular Fluid Dynamics* Bergel, D.H. (ed.), Vol. 1. Academic Press, New York, by permission.

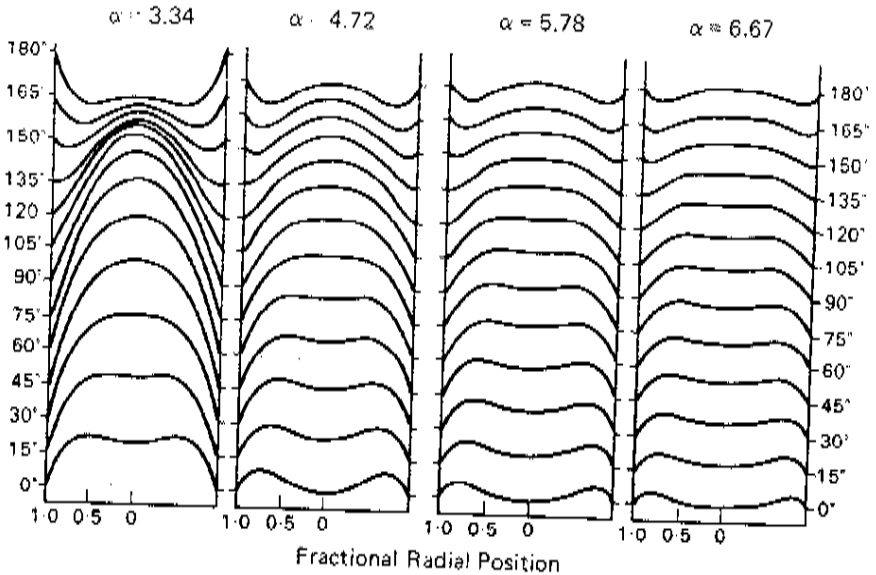

FIGURE 3.7.5. Theoretical velocity profiles of a sinusoidally oscillating flow in a pipe, with the pressure gradient varying as $\cos \omega t$. α is the Womersley number. Profiles are plotted for phase angle steps of $\Delta\omega t = 15°$. For $\omega t > 180°$, the velocity profiles are of the same form but opposite in sign. From McDonald (1974), by permission.

profiles are seen to become flatter and flatter in the central portion of the tube.

Problems

3.10 The total volume rate of flow in all generations of blood vessels is the same. In which vessels is the Reynolds number the largest in the human and dog?

3.11 If the diameter of the aorta of a person is unusually small, would the blood flow be more likely to be laminar or turbulent? If cardiac output is the same but the heart rate is increased, would the blood flow be more likely to become turbulent?

3.12 Estimate the difference between the peak Reynolds number and the mean Reynolds number of blood flow in the aorta of the dog.

3.8 Wave Propagation in Blood Vessels

Before taking up the full complexity of pulse-wave propagation in arteries, let us consider some idealized cases and learn a few basic facts. Let us consider first an infinitely long, straight, isolated, circular, cylindrical, elastic